DOI: 10.1478/AAPP.103S2A1

AAPP | Atti della Accademia Peloritana dei Pericolanti
Classe di Scienze Fisiche, Matematiche e Naturali
ISSN 1825-1242

Vol. 103, No. S2, A1 (2025)

NEW DATA ABOUT GEOPHYSICAL SURVEY AT GROTTA DELLE VENERI (PARABITA, LECCE)

CHIARA TORRE [a*], LARA DE GIORGI [b], DORA FRANCESCA BARBOLLA [b] AND GIOVANNI LEUCCI [b]

ABSTRACT. In order to investigate the possible extension of a cave of great archaeological interest, integrated geophysical measurements have been undertaken. Electrical resistivity tomography (ERT) and ground-penetrating radar (GPR) have been used. The cave, called "Grotta delle Veneri" (Cave of the Venus), is located in the archaeological site of Parabita (Apulia, southern Italy). It is one of the most important archaeological constructions of the Salento peninsula since its discovery confirmed the presence of the Neanderthal man in the Mediterranean Basin. The results are surprising and show different areas with the presence of cavities in the vicinity of the same cave.

1. Introduction

The Grotta delle Veneri is located in a karstic area 40 Km south of Lecce, near the village of Parabita (Fig. 1). It lies on a ridge, elongated in the NNO-SSE direction, locally known as the *Serra di S. Eleuterio*, which is characterized by limestones and dolomitic limestones with thicknesses ranging from a few centimetres to about 1 m. To the east of the Serra, more recent sediments crop out on a flat surface widely covered by *terra rossa* deposits. They can be divided into: *Calcareniti of Salento*, consisting of coarse calcarenites from the Lower Pleistocene; Sub-Apennine Clays, made of clay deposits from the Lower Pleistocene and terraced marine beach and flat coastal deposits from the Middle-Upper Pleistocene.

The presence of humans in the territory of Parabita dates back to 80.000 B.C. In fact, an artefact of Homo Sapiens Neanderthalensis (Neanderthal) and one of Homo Sapiens-Sapiens (Cro-Magnon) (35,000-10,000 B.C.) have been recovered in the cave *Grotta delle Veneri* in 1966. Two statuettes (2.000-10.000 B.C.) representing two pregnant women have been found in the same year.

The *Grotta delle Veneri* (Cave of the Venus) is one of the most important archaeological installations of the Salento peninsula, since its discovery confirmed the presence of the Neanderthal man in the Mediterranean Basin. Karst areas are the subject of several studies in

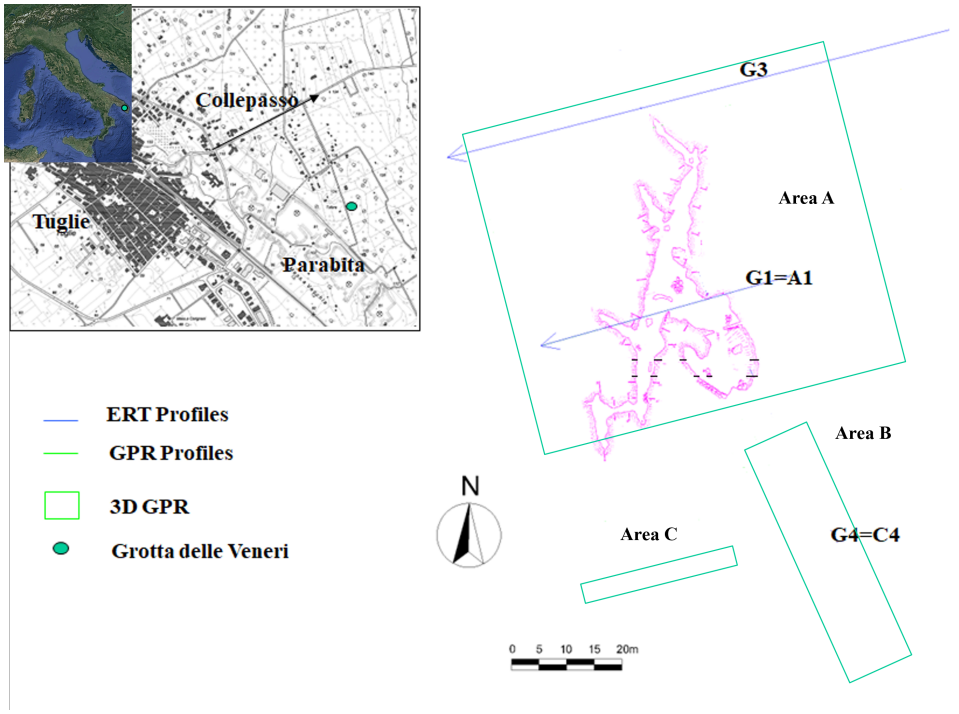

FIGURE 1. Investigated areas

the fields of archaeology, environment, hydrogeology, geology and geomorphology (Smith, 1986; Leucci and De Giorgi, 2005; Nuzzo et al., 2007; Carrozzo et al., 2008; Leucci and De Giorgi, 2010; Delle Rose and Leucci, 2010; Chalikakis et al., 2011; Abbas et al., 2012; Martinez-Moreno et al., 2013; De Giorgi and Leucci, 2014; Leucci and De Giorgi, 2015; Leucci et al., 2015; Leucci et al., 2016; Lapenna et al., 2017; Abidi et al., 2018; Pazzi et al., 2018; Hussain et al., 2020).

Non-invasive and high-resolution geophysical methods are appropriate for identifying and mapping the subsurface karst features (Leucci and De Giorgi, 2010; Hussian et al., 2020). The contrast created in the physical properties in comparison to the surrounding rocks, when the natural cavities are filled with water, air or collapsed materials, can be detected with the application of geophysical methods (Leucci and De Giorgi, 2010; Leucci and De Giorgi, 2015). A variety of geophysical methods are commonly employed to delineate buried karst features, including Ground Penetrating Radar (GPR), Electrical Resistivity Tomography (ERT), and gravimetry. (Leucci and De Giorgi, 2010; Leucci and De Giorgi, 2015).

The Grotta delle Veneri has been studied by Leucci and De Giorgi (2005 and 2015), who investigated its stability conditions using ERT, GPR and 3D seismic methods. The present study aims to detect potential cavities potentially related to an extension of the Grotta della Veneri. Two geophysical techniques, Electrical Resistivity Tomography (ERT) and Ground Penetrating Radar (GPR), have been used. Geophysical investigations have

been conducted in three distinct areas, designated as Areas A, B and C (Fig. 1). The terrain configuration, characterized by obstacles and slopes, restricted the investigation to these locations. 3D GPR measurements have been carried out across all three areas, while only three 2D ERT profiles could be acquired. This non-invasive characterization of the site is crucial for archaeologists to identify cavities for further excavations. The results provide a solid basis and recommendations for future investigation aimed at enhancing our knowledge about the frequentation of primitive man in the area.

2. Materials and Methods

2.1. Electrical Resistivity Tomography. The ERT method consists of injecting current (I) into the subsoil through two electrodes (called A and B) located on the surface. The potential difference (V) is measured by two others electrodes (called M and N). The apparent resistivity ρ, obtained from Ohm's law, is given by

$$\rho = K \cdot \frac{V}{I} \tag{1}$$

where K, called geometric factor, depends on the geometric arrangement of the electrodes; in general, it is expressed by the equation

$$K = 2\pi \left| \frac{1}{AM} - \frac{1}{AN} - \frac{1}{BM} - \frac{1}{BN} \right| \tag{2}$$

which can take more simplified forms depending on the geometric arrangement of the electrodes used in the geoelectrical survey. The various configurations differ only in the position of the electrodes (Loke, 2001; Leucci, 2019; Leucci, 2020).

ERT data have been acquired using the Syscal R1 Geo Resistivity Meter (Iris Instruments). A total of 48 electrodes have been employed with an interelectrode distance of 1 m for profiles G1 and G4, and of 2 m for profile G3 (Fig. 1). Profiles G1 and G4 are spatially superimposed on GPR profiles A1 and C4 respectively (Fig. 1). The dipole-dipole array has been used in order to obtain a much more detailed image of the subsurface, which is essentially composed of a highly inhomogeneous overburden and a bedrock (Loke 2001). All the field data have been processed using the RES2DINV software which allowed the *last squares* type inversion to be performed (Loke and Barker, 1996).

2.2. GPR survey. The Ground Penetrating Radar (GPR), also known as Georadar, is one of the most widely accepted and used geophysical methods for shallow subsurface exploration (Giannino and Leucci 2022). The GPR technique consists of transmitting an electromagnetic wave of an assigned frequency, via a transmitting antenna, and receiving the electromagnetic wave that has been reflected to the surface, via a receiving antenna. The reflection of the electromagnetic wave is only possible of bodies with different dielectric properties (Davis et al., 1989).

The time elapsing between the input of the electromagnetic pulse into the ground and the reception of the reflected one makes it possible to derive the depth of the reflecting surface if the electromagnetic waves propagation velocity in the medium is known. It is worth noting that electromagnetic waves propagate very well in the vacuum and less well in the

matter. They are sometimes absorbed even by very thin layers: the GPR method therefore only allows the subsurface to be investigated over small thicknesses (of the order of a few tens of metres).

Other factors that must be considered in the study of the electromagnetic wave propagation are the penetration depth and the resolution. The penetration depth decreases as the frequency increases, while radar resolution increases with higher frequencies (Giannino and Leucci, 2022). Both of them are influenced by the mineralogical characteristics of the medium investigated, mainly by its clay and water content, as well as by the surface vegetation and soil morphology.

The frequencies of the electromagnetic pulses used vary from a few MHz to a few GHz. The wavelength (λ), frequency (f) and propagation velocity (v) of electromagnetic pulse are linked by the following equation

$$\lambda = \frac{v}{f} \tag{3}$$

Once the frequency to be used in the geophysical survey has been chosen and the velocity of propagation in the medium is known, the equation (3) allows the wavelength to be derived and thus the resolving power of the electromagnetic survey to be estimated.

It is obvious that, for the same v, as the frequency increases, the resolving power increases. It is also known that as the frequency increases, the absorption power of the medium increases and thus the penetration depth decreases. This absorption also depends on the conductivity of the dielectric medium, which is mainly regulated by the content of water and salts in solution.

In the two-dimensional radar sections, the positions of the antennas along the investigated profile are shown on the abscissa, while the two-way travel times—i.e., the time between the emission of the impulse and the reception of the reflected signal at the surface—are shown on the ordinate. These reflections correspond to subsurface discontinuity surfaces.

A GPR investigation has been carried out using the Sir System 2 georadar (GSSI) and the 200 MHz antenna. In Area A (36 m × 50 m), 37 parallel profiles spaced 1 m apart were acquired along the x-direction, and 3 parallel profiles spaced 1 m apart were acquired along the y-direction. In Area B (10 m × 40 m), 11 parallel profiles spaced 1 m apart were collected along the x-direction. In Area C (3 m × 20 m), 4 parallel profiles spaced 1 m apart were acquired along the x-direction. The acquisition parameters were: 512 samples per scan, a time window of 150 ns and manual gain. Data have been processed using a GPR-SLICE software. processing steps included:

- Time-zero drift correction;
- Background removal algorithm with a mean of traces without strong targets;
- Amplitude analysis and gain function;
- Band-pass filter;
- f-k migration;
- Time slices generation;
- Amplitude isosurfaces cube generation.

In order to estimate the average electromagnetic wave velocity of the investigated site, the hyperbolic diffraction method has been used. The average velocity was found 0.09 m/ns.

3. Data analysis and Results

3.1. GPR survey.

3.1.1. *Area A*

From an analysis of the radar sections, an example of which is shown in Fig. 2, it was observed:

a. the presence of a series of hyperbolic-shaped anomalies (labelled A) of great extension, the upper portion of which lies between 20 ns and 60 ns (0.9 m - 2.7 m depth), characterised by a very high signal amplitude. Their dimensions are of the order of 8-10 m and are spatially organised; for this reason, they have been interpreted as part of the Cave of Venus.

b. a series of hyperbolic-shaped anomalies (labelled B) of limited extension, the upper portion of which is in a range between 50 ns and 80 ns (2.25 m - 3.6 m depth). Their dimensions are of the order of 0.5 - 1 m. They have therefore been interpreted as characterising a highly fractured rocky basement below the cave.

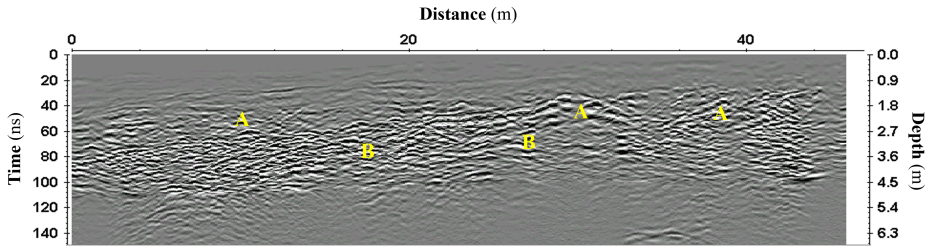

FIGURE 2. Area A: radar section relating to profile A1

The planimetric position of the profiles made it possible to spatially correlate the anomalies present on each georadar profile using the amplitude analysis of the reflected events within assigned time intervals (time slice) (Fig. 3) (Giannino and Leucci, 2022).

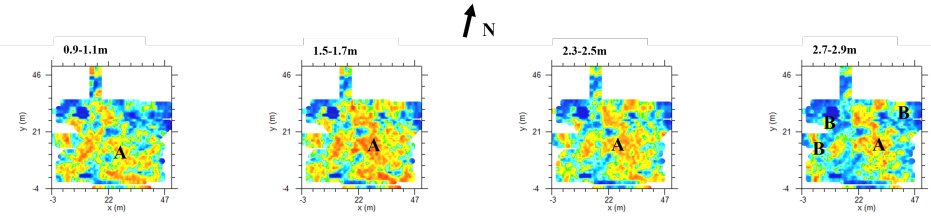

FIGURE 3. Area A: time slices

As it is well known, the amplitude of reflected events is directly correlated with the contrast between the electrical characteristics of the media in the subsurface. Therefore,

the three-dimensional visualisation, by amplitude intervals, of the distribution of reflected events allows the spatial localisation of the structures that determine the reflections. Each time slice corresponds to a layer of soil whose depth and thickness depend not only on the values assumed for time but also on the propagation velocity of the electromagnetic waves in the subsoil. Time slices have been calculated at soil thickness intervals of 0.2 m.

Fig. 3 shows the most significant time slices. The representation in time slices has better defined the most intense anomalies (A in Fig. 2). A clear main alignment of the reflection indicated with A is indicative of the presence of cavities between at least 0.9 - 2.7 m depth. The presence of scattered high amplitude anomalies throughout the rest of the slice, indicated with B, confirms the hypothesis of a strongly fractured basement. The amplitude isosurfaces (Fig. 4) help to better understand the position of the cavity in a 3D way.

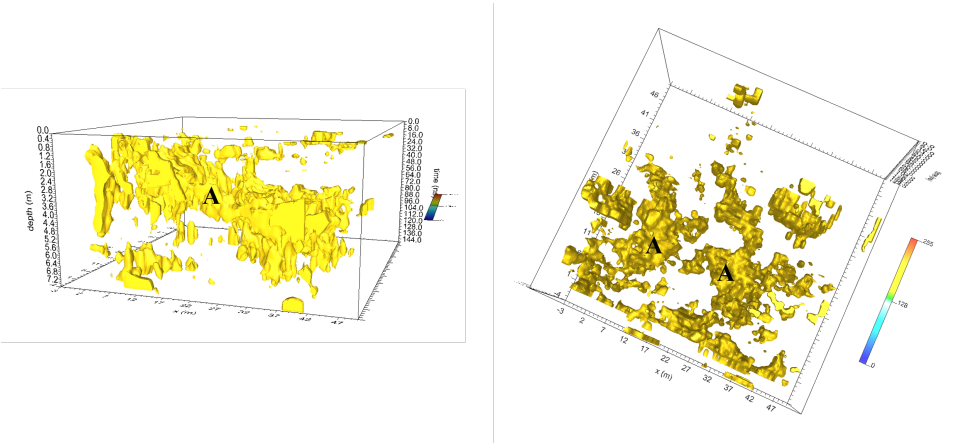

FIGURE 4. Area A: amplitude isosurfaces

3.1.2. *Area B*

From the analysis of the radar sections, an example of which is shown in Fig. 5, the following was observed: the presence of an area (E), between the abscissae 0 - 6 m, in which the radar signal is strongly absorbed, indicating a highly conductive material; hyperbolic-shaped anomalies (indicated by C), between the abscissae 8 - 35 m, whose upper part is between 40 ns and 80 ns (1.8 m - 3.6 m depth), characterised by a very high signal amplitude, indicating a probable presence of a cavity that is not completely empty or a very heavily fractured area.

Time slices (Fig. 6) show the presence of a zone with a strong absorption of the radar signal (E) and the presence of a probable cavity (C).

The amplitude isosurfaces (Fig. 7) help to better understand the position of the cavity in a 3D way.

3.1.3. *Area C* The analysis of the processed radar sections, an example of which is shown in Fig. 8, revealed: the presence of a series of hyperbolic anomalies (D), the upper part

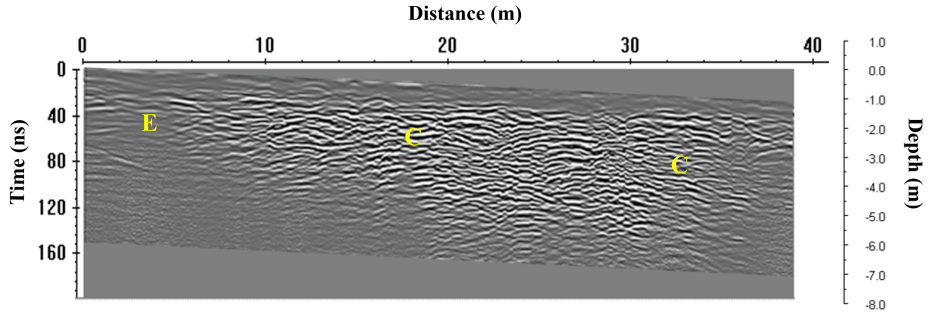

FIGURE 5. Area B: radar section relating to profile C4

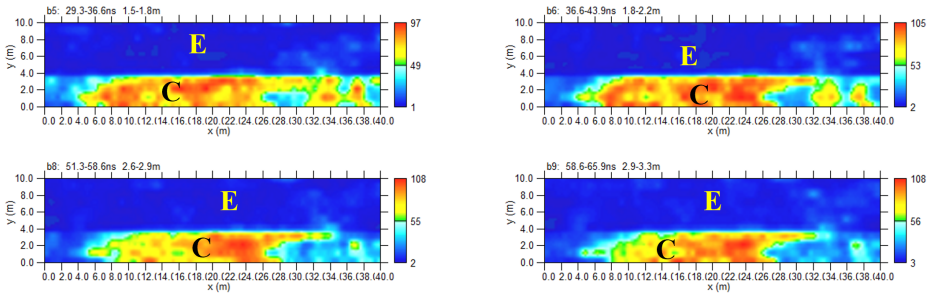

FIGURE 6. Area B: time slices

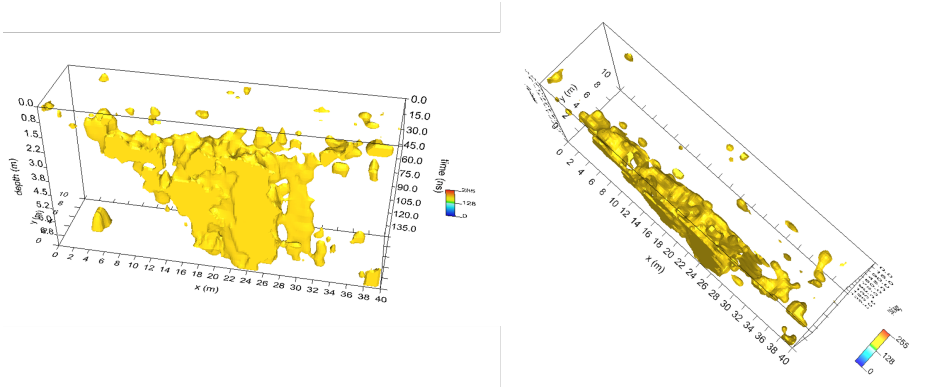

FIGURE 7. Area B: amplitude isosurfaces

of which lies between 20 ns and 80 ns (0.9 m - 3.6 m depth), characterised by a very high

signal amplitude. They are of the order of 4.0-5.0 m in size and are spatially organised, which is why they have been interpreted as probable cavities.

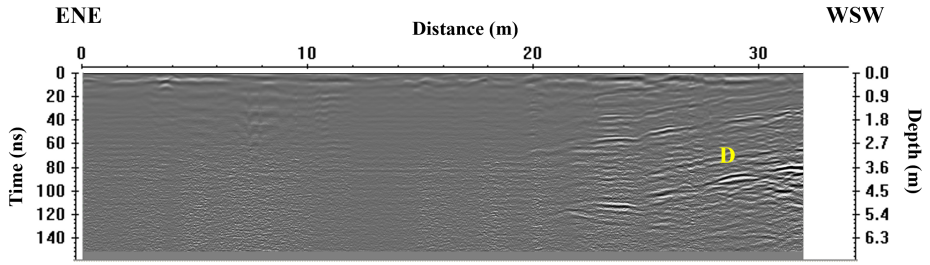

FIGURE 8. Radar section of the data acquired in area C

Time slices (Fig 9) show the presence of an area related to the probable presence of a cavity (D).

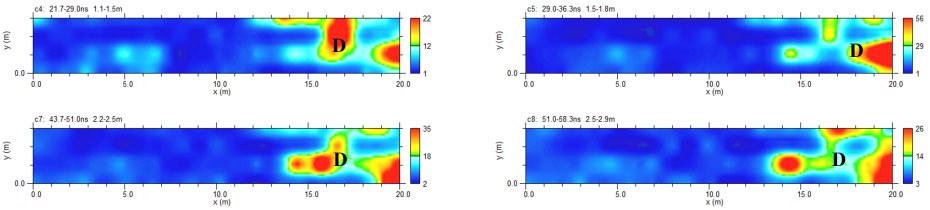

FIGURE 9. Area C: time slices

The amplitude isosurfaces (Fig. 10) help to better understand the position of the cavity in a 3D way.

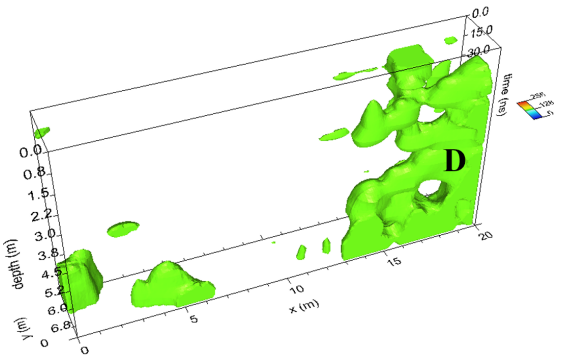

FIGURE 10. Area C: amplitude isosurfaces

3.2. Electrical resistivity tomography (ERT) survey. The 2D resistivity distribution in the subsurface is shown in figs. 11, 12 and 13.

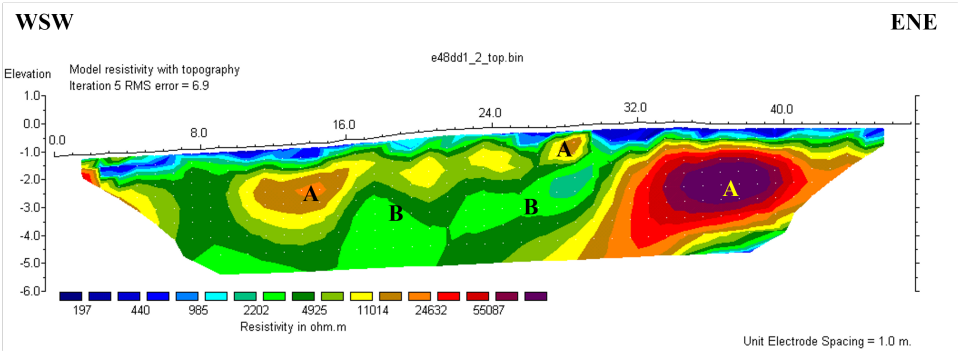

FIGURE 11. Geoelectrical profile G1

Fig. 11 shows a series of anomalies (indicated with A) whose roof is located at a depth of approximately 1 m, with a resistivity more than 10000 $\Omega \cdot m$ associated with the presence of cavities. Various anomalies (indicated with B), whose roof is located at a depth of between 1 m and 3 m, have a resistivity of between 2000 and 3000 $\Omega \cdot m$, confirming the presence of voids and strongly fractured material.

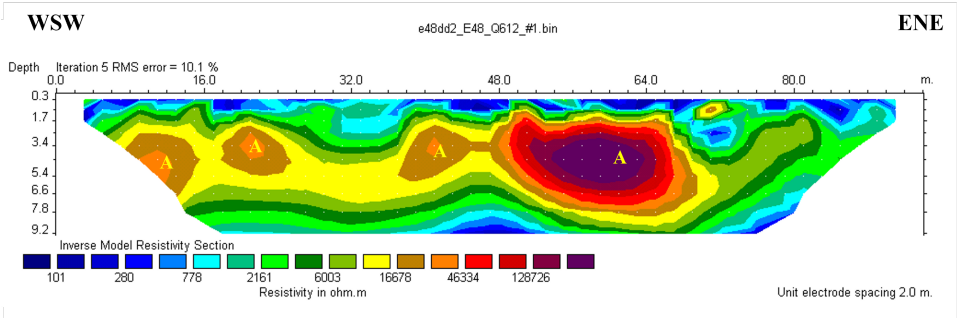

FIGURE 12. Geoelectrical profile G3

The profile G3 (Fig. 12) revealed a series of anomalies (indicated with A) whose roof is located at a depth of approximately 1.5 m and whose resistivity exceeds 22000 $\Omega \cdot m$, which can also be associated with cavities. In particular, the most extensive anomaly, between the abscissae 28 - 46 m, could be associated with a north - east extension of the cave itself.

The profile G4 (Fig. 13) shows an area, between the abscissae 0 - 20 m (denoted by F), of strongly conductive material with resistivities between 20 and 50 $\Omega \cdot m$; a series of anomalies (indicated with E) whose roof is located at a depth of approximately 2 m, of variable extension, and resistivities between 2000 and 4000 $\Omega \cdot m$ indicating the presence of probably voids; an anomaly (indicated with C), whose roof of which is located at a depth of

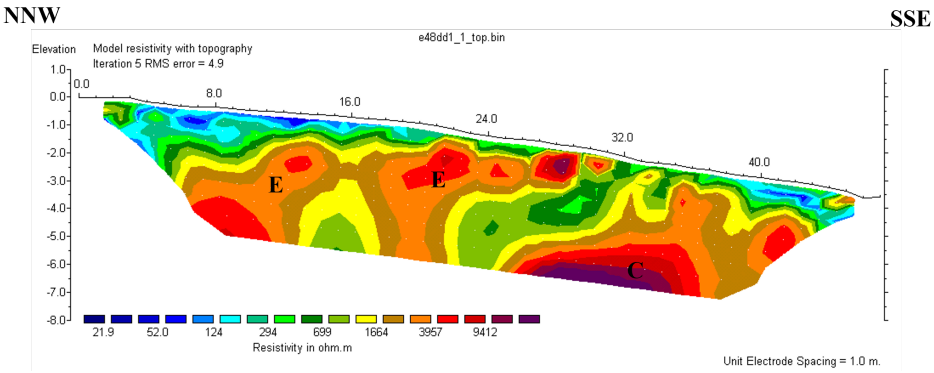

FIGURE 13. Geoelectric profile G4

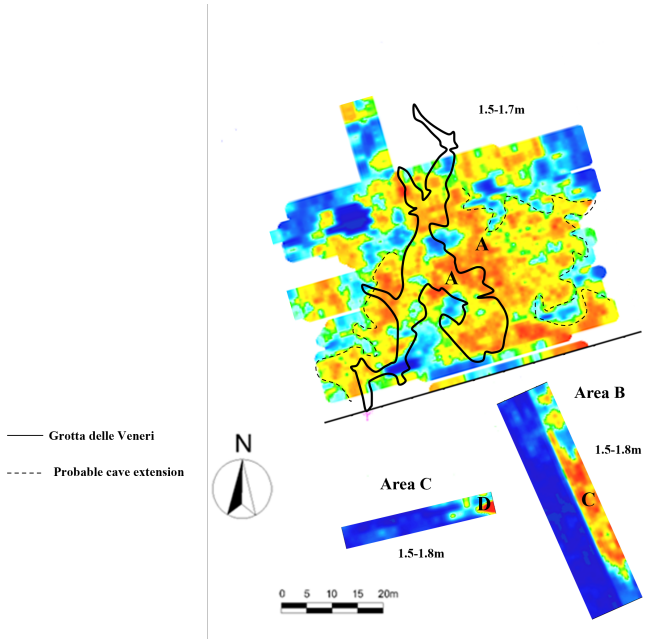

FIGURE 14. Summary map of results obtained with the georadar survey

approximately 4 m, with resistivity greater than 9000 $\Omega \cdot m$ indicating the probable presence of a cavity.

4. Conclusions

The geophysical investigations partially covered the area of the Grotta delle Veneri. The summary results of the campaign data are shown in Figs. 14 and 15.

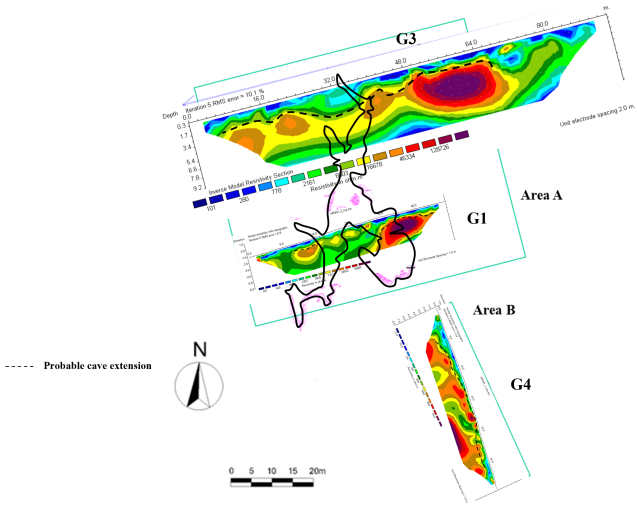

FIGURE 15. Summary map of results obtained from the geoelectric survey. The G3, G1 and G4 profiles have to be considered in the X-Z plane, while the map of the Grotta delle Veneri and areas investigated are shown in the X-Y plane

It can be assumed that all or most of the anomalies can be related to the probable presence of caves. In the surveyed areas, the anomalies present in the two-dimensional radar sections that appear aligned in time slices are probably related to a part of the cave and seem to have a cave extension. The result of the geoelectrical survey seems to confirm these findings.

The non-invasive aspects of these investigations and the results obtained are crucial for archaeologists to plan future investigations in order to enhance knowledge of early human habitation in the area.

References

Abdelfattah, A., Demehati, A., Banouni, H., and El Qandil, M. (2018). "The Importance of Underground Cavities Detection in the Choice of Constructible Areas: Case of the Agglomeration of Fez (Morocco)". *Geotechnical and Geological Engineering* **36**, 1919–1932. DOI: 10.1007/s10706-017-0425-3.

Ali, A., Khalil, M., Massoud, U., Santos, F. M., Mesbah, H., Lethy, A., Soliman, M., and Ragab, E. S. A. (2012). "The implementation of multi-task geophysical survey to locate Cleopatra Tomb at Tap-Osiris Magna, Borg El-Arab, Alexandria, Egypt "Phase II"". *NRIAG Journal of Astronomy and Geophysics* **1**, 1–11. DOI: 10.1016/j.nrjag.2012.11.001.

Argentieri, A., Carluccio, R., Cecchini, F., Chiappini, M., Ciotoli, G., De Ritis, R., Di Filippo, M., Di Nezza, M., Marchetti, M., Margottini, S., Materni, V., Meloni, F., Nardi, A., Rotella, G., Sapia, V., and Venuti, A. (2015). "Early stage sinkhole formation in the Acque Albule basin of central Italy from geophysical and geochemical observations". *Engineering Geology* **191**, 36–47. DOI: 10.1016/j.enggeo.2015.03.010.

Carrozzo, M. T., Leucci, G., Margiotta, S., Mazzone, F., and Negri, S. (2008). "Integrated geophysical and geological investigations applied to sedimentary rock mass characterization". *Annals of Geophysics* **51**, 191–202. DOI: 10.4401/ag-3044.

Chalikakis, K., Plagnes, V., Guérin, R., Valois, R., and Bosch, F. P. (2011). "Contribution of geophysical methods to karst-system exploration: An overview". *Hydrogeology Journal* **19**, 1169–1180. DOI: 10.1007/s10040-011-0746-x.

Conyers, L. and Goodman, D. (1997). *Ground-penetrating Radar: An Introduction for Archaeologists*. G - Reference, Information and Interdisciplinary Subjects Series. AltaMira Press. URL: https://books.google.fr/books?id=hjBmAAAAMAAJ.

Davis, J. and Annan, A. P. (1989). "Ground penetrating radar for high-resolution mapping of soil and rock stratigraphy. Geophysical Prospecting 37, 531-551". *Geophysical Prospecting* **37**, 531–551. DOI: 10.1111/j.1365-2478.1989.tb02221.x.

De Giorgi, L. and Leucci, G. (2014). "Detection of Hazardous Cavities Below a Road Using Combined Geophysical Methods". *Surveys in Geophysics* **35**, 1003–1021. DOI: 10.1007/s10712-013-9277-4.

Delle Rose, M. and Leucci, G. (2010). "Towards an integrated approach for characterization of sinkhole hazards in urban environments: The unstable coastal site of Casalabate, Lecce, Italy". *Journal of Geophysics and Engineering* **7**, 143–154. DOI: 10.1088/1742-2132/7/2/004.

Ezersky, M. (2008). "Geoelectric structure of the Ein Gedi sinkhole occurrence site at the Dead Sea shore in Israel". *Journal of Applied Geophysics - J APPL GEOPHYS* **64**, 56–69. DOI: 10.1016/j.jappgeo.2007.12.003.

Giannino, F. and Leucci, G. (2021). *Electromagnetic Methods in Geophysics: Applications in GeoRadar, FDEM, TDEM, and AEM*. Wiley. URL: https://books.google.fr/books?id=OnpAEAAAQBAJ.

Hussain, Y., Uagoda, R., Borges, W., Nunes, J. G. S., Hamza, O., Condori, C., Aslam, K., Dou, J., and Cárdenas-Soto, M. (2020). "The Potential Use of Geophysical Methods to Identify Cavities, Sinkholes and Pathways for Water Infiltration". *Water*, 2289. DOI: 10.3390/w12082289.

Krawczyk, C. M., Polom, U., Trabs, S., and Dahm, T. (2012). "Sinkholes in the city of Hamburg-New urban shear-wave reflection seismic system enables high-resolution imaging of subrosion structures". *Journal of Applied Geophysics - J APPL GEOPHYS* **78**, 133–143. DOI: 10.1016/j.jappgeo.2011.02.003.

Lapenna, V., Leucci, G., Parise, M., Porfyriou, H., Genovese, L., and Varriale, R. (2017). "A project to exploit the importance of the natural and cultural heritage of the underground environment in southern Italy". *Proceedings of International Congress of Speleology in Artificial Cavities - Cappadocia, 6-8/04/2017*. URL: https://books.google.fr/books?id=hjBmAAAAMAAJ.

Leucci, G. and De Giorgi, L. (2005). "Integrated geophysical surveys to assess the structural conditions of a karstic cave of archaeological importance". *Natural Hazards and Earth System Science* **5**, 17–22. DOI: 10.5194/nhess-5-17-2005.

Leucci, G. and De Giorgi, L. (2010). "Microgravimetric and ground penetrating radar geophysical methods to map the shallow karstic cavities network in a coastal area (Marina Di Capilungo, Lecce, Italy)". *Exploration Geophysics* **41**, 178–188. DOI: 10.1071/EG09029.

Leucci, G. and De Giorgi, L. (2015). "2D and 3D seismic measurements to evaluate the collapse risk of an important prehistoric cave in soft carbonate rock". *Open Geosciences* **7**, 84–94. DOI: 10.1515/geo-2015-0006.

Leucci, G., De Giorgi, L., and Delle Rose, M. (2016). "The Sinkhole Hazard Study at Casalabate (Lecce, Italy) using Geophysical and Geological Surveys". *International Journal of Engineering Research and Science* **2**, 71–81. URL: https://ijoer.com/assets/articles_menuscripts/file/IJOER-JAN-2016-21.pdf.

Loke, M. H. (2000). *Electrical imaging surveys for environmental and engineering studies, A practical guide to 2-D and 3-D surveys: RES2DINV Manual*.

Martínez-Moreno, F. J., Pedrera, A., Ruano, P., Galindo-Zaldivar, J., Martos-Rosillo, S., Gonzalez Castillo, L. C., Sánchez-Úbeda, J. P., and Marín-Lechado, C. (2013). "Combined microgravity, electrical resistivity tomography and induced polarization to detect deeply buried caves: Algaidilla cave (Southern Spain)". *Engineering Geology* **162**, 67–78. DOI: 10.1016/j.enggeo.2013.05.008.

Nuzzo, L., Leucci, G., and Negri, S. (2007). "GPR, VES and refraction seismic surveys in the karstic area "Spedicaturo" near Nociglia (Lecce, Italy)". *Near Surface Geophysics* **5**(1), 67–76. URL: https://www.earthdoc.org/content/journals/10.3997/1873-0604.2006019.

Pazzi, V., Filippo, M., Di Nezza, M., Carlà, T., Bardi, F., Marini, F., Fontanelli, K., Intrieri, E., and Fanti, R. (2018). "Integrated geophysical survey in a sinkhole-prone area: Microgravity, electrical resistivity tomographies, and seismic noise measurements to delimit its extension". *Engineering Geology* **243**, 282–293. DOI: 10.1016/j.enggeo.2018.07.016.

Smith, D. L. (1986). "Application of the pole-dipole resistivity technique to the detection of solution cavities beneath highways". *Geophysics* **51**(3), 833–837. DOI: 10.1190/1.1442135.

Al-Tarazi, E., Rajab, J. A., El-Naqa, A., Elwaheidi, M. M., and Al-Tarazi, E. (2008). "Detecting leachate plumes and groundwater pollution at Ruseifa municipal landfill utilizing VLF-EM method". *Journal of Applied Geophysics* **65**, 121–131. DOI: 10.1016/j.jappgeo.2008.06.005.

Zhou, W., Beck, B. F., and Adams, A. L. (2002). "Effective electrode array in mapping karst hazards in electrical resistivity tomography". *Environmental Geology* **42**, 922–928. DOI: 10.1007/s00254-002-0594-z.

---

[a] University of Malta, Department of Geosciences
[b] Istituto di Scienze del Patrimonio Culturale - CNR

* To whom correspondence should be addressed | email: chiara.torre@um.edu.mt

Paper contributed to the XII *Congresso Nazionale della Associazione Italiana di Archeometria* held in Messina, Italy (19-21 April 2023) under the patronage of the *Accademia Peloritana dei Pericolanti*.

Manuscript received 24 January 2024; published online 12 December 2025